

## Supplemental Information

# Proteomics and Molecular Network Analyses Reveal that the Interaction between the TAT-DCF1 Peptide and TAF6 Induces an Antitumor Effect in Glioma Cells

Jiao Wang<sup>a</sup>, Fushuai Wang<sup>a</sup>, Qian Li<sup>a</sup>, Qian Wang<sup>a</sup>, Jie Li<sup>a</sup>, Yajiang Wang<sup>a</sup>, Jiamin Sun<sup>b</sup>,  
Dongfang Lu<sup>b</sup>, Hong Zhou<sup>a</sup>, Shiman Li<sup>a</sup>, Sujuan Ma<sup>c</sup>, Jiang Xie<sup>b,\*</sup>, Tieqiao Wen<sup>a,\*</sup>

**Table S1**

Project	Contents
Data Acquisition Software	Thermo Xcalibur 4.0 (Thermo, USA)
Reversed phase column information	C18 column (75μm x 25cm, Thermo, USA)
Chromatography instrument	EASY-nLC 1200
Mass Spectrometer	Q-Exactive (Thermo, USA)
Chromatographic separation time	90min      A : 2% ACNwith 0.1% formic acid B: 80% ACN with 0.1% formic acid
Flow rate	300nL/min
Gradient [Time(min)/B(%)]	0/2,70/40,70.1/90,75/90,75.1/2,90/2
MS scan range (m/z)	350-1300
Acquisition mode	DDA
First-order mass spectrometry resolution	7000
Fragmentation mode	HCD
Secondary resolution	17500

Dynamic exclusion time(s) 18

---

**Table S1. Liquid chromatography tandem mass spectrometry parameters**

**Table S2**

---

Gene name	Primer sequence (5' to 3')
<i>DCFI</i>	Upstream : CCTACCCCTTGCACACCTAC Downstream : GGGACATGAGTTGTTCTTGTCTC
<i>TAF6</i>	Upstream : GCACATGGGGAAACGACAGAA Downstream : CTTCAAGGCGTAGTCAATGTCA
<i>RPS27A</i>	Upstream : CTCGAGGTTGAACCCTCGGA Downstream : CTGATCAGGAGGAATTCTTCC
<i>TRAF6</i>	Upstream : CATGCCCTGGATTCTACAC Downstream : TCTCCTTGCATTGTGTGGAC
<i>HMGB1</i>	Upstream : AAGAAGTGCTCAGAGAGGTGGAAG Downstream : GAAGAAGGCCGAAGGAGGCCTCTT
<i>HMGB2</i>	Upstream : CGGGCAAAATGTCCTCGTA Downstream : GCAGACATGGTCTTCATCTCTC
<i>TOP2</i>	Upstream : TGGCTGTGGTATTGTAGAAAGC Downstream : TTGGCATCATCGAGTTGGGA
<i>GAPDH</i>	Upstream : TCACCACCATGGAGAAGGC Downstream : GCTAACAGTTGGTGGTGCA

---

**Table S2.List of the primers used for qPCR**

**Table S3**

Function	P-value	Genes in the predicted signaling network
<u>SRP-dependent cotranslational protein targeting to membrane</u>	$8.89 \times 10^{-40}$	<i>RPL18, RPL17, RPL14, RPL15, RPS15A, RPLP2, RPL36, RPS2, RPS3, RPS25, RPL30, RPL7, RPL32, RPL31, RPS3A, RPLP0, RPL34, RPL8, FAU, RPL10A, RPL7A, RPS20, RPL12, RPS21, RPS24, RPSA, RPL24, RPL23A, RPS8, RPL29, RPS18, RPS19, RPS16, RPL18A, RPL22, RPL13A, RPS14, RPS10, UBA52</i>
<u>translational initiation</u>	$1.34 \times 10^{-36}$	<i>RPL18, RPL17, RPL14, RPL15, RPS15A, RPLP2, RPL36, RPS2, RPS3, RPS25, RPL30, RPL7, RPL32, RPS3A, RPL31, RPLP0, RPL34, EIF1AY, RPL8, FAU, RPL10A, RPL7A, RPS20, RPL12, RPS21, RPS24, RPSA, RPL24, RPL23A, RPS8, RPL29, RPS18, RPS19, RPS16, RPL18A, RPL22, RPL13A, RPS14, EIF2S1, EIF4A1, RPS10, UBA52</i>
viral transcription	$2.49 \times 10^{-36}$	<i>RPL18, RPL17, RPL14, RPL15, RPS15A, RPLP2, RPL36, RPS2, RPS3, RPS25, RPL30, RPL7, RPL32, RPL31, RPS3A, RPLP0, RPL34, RPL8, FAU, RPL10A, RPL7A, RPS20, RPL12, RPS21, RPS24, RPSA, RPL24, RPL23A, RPS8, RPL29, RPS18, RPS19, RPS16, RPL18A, RPL22, RPL13A, RPS14, RPS10, UBA52</i>
nuclear-transcribed mRNA catabolic process, nonsense-mediated decay	$3.52 \times 10^{-35}$	<i>RPL18, RPL17, RPL14, RPL15, RPS15A, RPLP2, RPL36, RPS2, RPS3, RPS25, RPL30, RPL7, RPL32, RPL31, RPS3A, RPLP0, RPL34, RPL8, FAU, RPL10A, RPL7A, RPS20, RPL12, RPS21, RPS24, RPSA, RPL24, RPL23A, RPS8, RPL29, RPS18, RPS19, RPS16, RPL18A, RPL22, RPL13A, RPS14, RPS10, UBA52</i>

		<i>RPL18, RPL17, RPL14, RPL15, RPS15A, RPLP2,</i>
		<i>RPL36, RPS2, RPS3, RPS25, RPL30, RPL7, RPL32,</i>
		<i>RPL31, RPS3A, RPLP0, RPL34, RPL8, SLC25A3, FAU,</i>
translation	$3.23 \times 10^{-26}$	<i>RPL10A, RPL7A, RPS20, RPL12, RPS21, RPS24,</i>
		<i>RPS4, SLC25A5, RRBPI, SLC25A6, RPL24, RPL23A,</i>
		<i>RPS8, RPL29, RPS18, RPS19, RPS16, RPL18A, RPL22,</i>
		<i>RPL13A, RPS14, RPS10, UBA52</i>
		<i>RPL18, RPL17, RPL14, RPL15, RPS15A, RPLP2,</i>
		<i>RPL36, RPS2, RPS3, RPS25, RPL30, RPL7, RPL32,</i>
rRNA processing	$5.80 \times 10^{-26}$	<i>RPL31, RPS3A, RPLP0, RPL34, RPL8, FAU, RPL10A,</i>
		<i>RPL7A, RPS20, RPL12, RPS21, RPS24, RPS4, RPL24,</i>
		<i>RPL23A, RPS8, RPL29, RPS18, PA2G4, RPS19, RPS16,</i>
		<i>RPL18A, RPL22, RPL13A, RPS14, RPS10, UBA52</i>
		<i>HSP90AB1, RPL14, CHMP4B, RPL15, CAPZA1,</i>
		<i>HIFX, RDX, RPS2, CAPZB, PRDX1, PKM, RACK1,</i>
		<i>CTTN, HNRNPK, MACF1, RPL34, LRRC59, RANBP1,</i>
cell-cell adhesion	$5.23 \times 10^{-24}$	<i>HSPA5, RPL7A, HSPA8, AHNAK, ENO1, BSG, RAN,</i>
		<i>FSCN1, RPL24, RPL23A, EEF2, FLNB, YWHAE,</i>
		<i>ANXA2, RPL29, EVPL, SERBPI, SPTBN2, TMOD3,</i>
		<i>EEF1G, SPTBN1, DBN1, PUF60, SPTANI</i>
movement of cell or subcellular component	$1.79 \times 10^{-11}$	<i>ACTB, CAPZA1, VIM, TPM1, CAPZB, TPM4, ACTG1,</i>
		<i>ACTR3, ARPC1B, ACTR2, TUBB, ARPC3, ARPC2,</i>
		<i>TXN, RAC1, MSN, TUBB4B</i>
mitochondrial ATP synthesis coupled proton transport	$1.36 \times 10^{-10}$	<i>ATP5B, ATP5F1, ATP5C1, STOML2, ATP5O, ATP5A1,</i>
		<i>ATP5I, COX5B, ATP5H, ATP5J</i>
cytoplasmic translation	$2.28 \times 10^{-8}$	<i>RPL7, RPL22, RPL31, RPLP0, RPL15, RPL8, RPL36,</i>
		<i>RPLP2, RPL29</i>

ATP biosynthetic process	$8.43 \times 10^{-8}$	<i>PKM, ATP5B, ATP5F1, ATP5C1, ATP5O, ATP5A1, ATP5I, ATP5H, ATP5J</i>
protein folding	$1.82 \times 10^{-7}$	<i>HSP90AB1, TMX1, HSP90AA1, GNAI3, GNAI2, PDIA3, PDIA6, LMAN1, CANX, TRAP1, HSP90B1, GNB2, PPIA, TXN, HSPE1, DNAJA3, HSPA8, HSPA9</i>
ATP synthesis coupled proton transport	$1.86 \times 10^{-7}$	<i>ATP5B, ATP5F1, ATP5C1, ATP6V0A1, ATP5O, ATP5A1, ATP5H, ATP5J</i>
cytoskeleton organization	$1.15 \times 10^{-6}$	<i>ACTB, CAPZB, TPM1, MAST3, KRT5, MACF1, KRT16, CFL1, AVIL, SPTBN2, SPTBN1, MSN, DST, TUBA1C, SPTAN1, TUBB4B</i>
ephrin receptor signaling pathway	$1.41 \times 10^{-6}$	<i>ACTB, ACTR3, ACTG1, CDC42, ACTR2, ARPC1B, ARPC3, ARPC2, RAC1, RHOA, MYL12A, YES1</i>
Arp2/3 complex-mediated actin nucleation	$4.00 \times 10^{-6}$	<i>ACTR3, ACTR2, ARPC1B, ARPC3, ARPC2, ARPC5L, ARPC4-TTLL3</i>
protein stabilization	$4.48 \times 10^{-6}$	<i>HSP90AB1, HSP90AA1, ATP1B3, FLOT2, PHB, CLU, NAA16, HSPA1B, FLNA, PPIB, PHB2, HSPD1, GAPDH, DNAJA3</i>
leukocyte migration	$7.78 \times 10^{-6}$	<i>CD47, SLC16A1, BSG, KRAS, ATP1B3, PROCR, PPIA, CD58, SHC1, MSN, MYH9, YES1, MIF</i>
Fc-gamma receptor signaling pathway involved in phagocytosis	$1.18 \times 10^{-5}$	<i>ACTB, HSP90AB1, HSP90AA1, MYOIC, ACTG1, ACTR3, ACTR2, ARPC1B, CDC42, ARPC3, ARPC2, RAC1, YES1</i>
hydrogen ion transmembrane transport	$3.27 \times 10^{-5}$	<i>COX7A2, UQCRC1, UQCRH, COX6B1, COX4II, COX7A2L, COX5A, COX6C, UQCRB</i>
mitochondrial electron transport, cytochrome c to oxygen	$4.22 \times 10^{-5}$	<i>COX6B1, COX4II, COX7A2L, COX5A, COX5B, COX6C</i>

viral process	$4.75 \times 10^{-5}$	<i>SLC25A5, RAN, VIM, HNRNPA1, YWHAE, VDAC1, RACK1, SET, HNRNPK, C1QBP, CENPA, NPM1, EIF4A1, RHOA, RANBP1, SHC1, HSPD1, RAB6A, HSPA8</i>
gene expression	$5.09 \times 10^{-5}$	<i>HNRNPA3, HNRNPK, HNRNPA2B1, HNRNPD, HNRNPH1, RBMX, HNRNPA1, HNRNPU</i>
substantia nigra development	$5.84 \times 10^{-5}$	<i>ACTB, CDC42, RHOA, ATP5F1, COX6B1, HSPA5, YWHAE, ATP5J</i>
actin filament capping	$1.07 \times 10^{-4}$	<i>GSN, AVIL, SPTBN2, SPTBN1, SPTAN1</i>
oxidative phosphorylation	$1.07 \times 10^{-4}$	<i>UQCRC2, UQCRC1, UQCRH, ATP5C1, UQCRB</i>
actin filament organization	$1.09 \times 10^{-4}$	<i>INPPL1, FSCN1, TMOD3, ACTN1, TPM2, CTNNAI, TPM1, DBN1, TPM4</i>
muscle filament sliding	$1.12 \times 10^{-4}$	<i>MYL6, ACTC1, NEB, VIM, TPM2, TPM1, TPM4</i>
membrane raft assembly	$1.63 \times 10^{-4}$	<i>FLOT2, FLOT1, S100A10, ANXA2</i>
platelet aggregation	$1.74 \times 10^{-4}$	<i>ACTB, ACTG1, ACTN1, MYL12A, MYH9, HBB, FLNA</i>
cell redox homeostasis	$1.76 \times 10^{-4}$	<i>P4HB, TMX1, PDI43, AIFM1, DLD, TXN, PDI46, PRDX3, PRDX1</i>
translational elongation	$4.22 \times 10^{-4}$	<i>TUFM, EEF1A1, EEF1G, RPLP2, EEF2</i>
positive regulation of substrate adhesion-dependent cell spreading	$4.48 \times 10^{-4}$	<i>CDC42, C1QBP, ARPC2, RAC1, S100A10, FLNA</i>
ER to Golgi vesicle-mediated transport	$4.67 \times 10^{-4}$	<i>CD55, CD59, ARF4, SPTBN2, TMED10, RAB1B, SPTBN1, LMAN1, NSF, GOLGB1, SPTAN1, BCAP31</i>
negative regulation of apoptotic process	$4.83 \times 10^{-4}$	<i>ACTC1, NAA16, PRDX3, FLNA, MIF, ATAD3A, HSP90B1, PA2G4, HNRNPK, RPS3A, ALB, PHB2, CD59, CFL1, NPM1, ARF4, HSPA5, HSPD1, MYO18A,</i>

		<i>UBA52, DNAJA3, HSPA9</i>
small GTPase mediated signal transduction	$5.73 \times 10^{-4}$	<i>RAB7A, HACD3, RAN, RAB5C, RAB1B, CDC42, KRAS, ARF4, RAC1, RHOA, RAB11A, RAPIA, RAB6B, RAB6A, DNAJA3</i>
mRNA splicing, via spliceosome	$6.86 \times 10^{-4}$	<i>FUS, HNRNPA2B1, RBMX, HNRNPA1, HNRNPU, PN, SRSF3, NONO, HNRNPA3, HNRNPK, DHX38, HNRNPD, HNRNPH1, HSPA8</i>
nucleosome assembly	$7.67 \times 10^{-4}$	<i>HIF0, HIST1H1E, HIST1H2BN, HIST1H1D, SET, HIST1H4A, HIST1H1C, CENPA, NPM1, HIFX</i>
response to endoplasmic reticulum stress	$8.57 \times 10^{-4}$	<i>P4HB, TMX1, HSP90B1, PDIA3, EIF2S1, FLOT1, PDIA6, EEF2</i>
mitochondrion organization	$1.00 \times 10^{-3}$	<i>SSBP1, PHB2, ATP5B, PHB, STOML2, PRDX3, PARP1, DNAJA3</i>
positive regulation of gene expression	$1.06 \times 10^{-3}$	<i>ACTC1, PHB, VIM, RDX, HSPA1B, HNRNPU, RPS3, CDC42, KRAS, EZR, RPS6KA2, GSN, HNRNPD, MSN, ZPR1</i>
actin cytoskeleton organization	$1.44 \times 10^{-3}$	<i>CDC42, KRAS, RAN, FSCN1, CFL1, RAC1, RHOA, TMOD3, FLNB, CAPZB</i>
retrograde vesicle-mediated transport, Golgi to ER	$1.45 \times 10^{-3}$	<i>ARF4, SURF4, TMED10, RAB1B, RAB6B, RAB6A, BICD2, NSF</i>
establishment of protein localization to plasma membrane	$1.60 \times 10^{-3}$	<i>JUP, EZR, FLOT2, FLOT1, S100A10, RDX</i>
canonical glycolysis	$1.81 \times 10^{-3}$	<i>PKM, TPII, HK1, GAPDH, ENO1</i>
protein folding in endoplasmic reticulum	$2.09 \times 10^{-3}$	<i>HSP90B1, PDIA3, HSPA5, CANX</i>

actomyosin structure organization	$2.09 \times 10^{-3}$	<i>EPB41L2, ACTC1, MYH9, MYO18A, MYH10</i>
adenine transport	$2.44 \times 10^{-3}$	<i>SLC25A5, SLC25A6, VDAC3</i>
regulation of organelle assembly	$2.44 \times 10^{-3}$	<i>EZR, RDX, MSN</i>
barbed-end actin filament capping	$2.62 \times 10^{-3}$	<i>GSN, CAPZA1, RDX, CAPZB</i>
actin cytoskeleton reorganization	$2.65 \times 10^{-3}$	<i>CTTN, EZR, RHOA, SHC1, MYH9, FLNA</i>
actin filament bundle assembly	$3.11 \times 10^{-3}$	<i>CDC42, EZR, ACTN4, FSCN1, ACTN1</i>
regulation of complement activation	$3.11 \times 10^{-3}$	<i>CD55, C1QBP, C4A, PHB2, CD59</i>
protein refolding	$3.23 \times 10^{-3}$	<i>HSP90AA1, HSPA1B, HSPD1, HSPA8</i>
mitochondrial electron transport, ubiquinol to cytochrome c	$3.23 \times 10^{-3}$	<i>UQCRC2, UQCRC1, UQCRH, UQCRB</i>
positive regulation of lamellipodium assembly	$3.91 \times 10^{-3}$	<i>HSP90AA1, ARPC2, FSCN1, RAC1</i>
establishment of endothelial barrier	$3.91 \times 10^{-3}$	<i>EZR, RAPIA, RDX, MSN</i>
ATP hydrolysis coupled proton transport	$3.96 \times 10^{-3}$	<i>ATP6API, ATP5B, ATP6V0A1, ATP1A1, ATP5A1</i>
maturation of SSU-rRNA from tricistronic rRNA transcript (SSU-rRNA, 5.8S rRNA, LSU-rRNA)	$3.96 \times 10^{-3}$	<i>RPS19, RPS16, RPS14, RPS8, RPS24</i>
positive regulation of protein localization to early endosome	$4.02 \times 10^{-3}$	<i>EZR, RDX, MSN</i>
aerobic respiration	$4.43 \times 10^{-3}$	<i>UQCRC2, UQCRC1, UQCRH, NDUFV1, UQCRB</i>

**Table S3. The top 61 most-enriched functions of the genes that have a *P*-value less than 0.05 in the predicted signaling network regulated by DCF1 in HEK293T-blank, where the**

**biological process from Gene Ontology was considered.**

**Table S4**

Function	P-value	Genes in the predicted signaling network
epidermis development	$4.75 \times 10^{-7}$	<i>KRT9, KRT17, KRT5, KRT16, CASP14, KRT14, KRT2, DSP</i>
intermediate filament organization	$1.59 \times 10^{-6}$	<i>KRT9, KRT17, VIM, KRT2, DSP</i>
establishment of skin barrier	$2.65 \times 10^{-6}$	<i>HRNR, FLG, KRT16, KRT1, FLG2</i>
keratinization	$6.99 \times 10^{-6}$	<i>HRNR, KRT17, KRT16, CASP14, KRT2, TGM3</i>
cytoskeleton organization	$3.33 \times 10^{-5}$	<i>ACTB, TUBA8, KRT6B, KRT5, APOE, KRT16, MSN, DST</i>
keratinocyte differentiation	$6.67 \times 10^{-5}$	<i>FLG, KRT16, DSP, TGM3, KRT10, CSTA</i>
intermediate filament cytoskeleton organization	$7.36 \times 10^{-5}$	<i>KRT6C, KRT6A, KRT16, DST</i>
cellular oxidant detoxification	$6.37 \times 10^{-4}$	<i>APOE, ALB, TXN, HBA1, HBB</i>
mitochondrion organization	$9.12 \times 10^{-4}$	<i>SSBP1, PHB2, ATP5B, PHB, PARP1</i>
protein stabilization	$9.98 \times 10^{-4}$	<i>LAMP1, PHB2, PHB, DSG1, HSPD1, GAPDH</i>
movement of cell or subcellular component	$1.38 \times 10^{-3}$	<i>ACTB, TUBB, VIM, TXN, MSN</i>
retina homeostasis	$1.44 \times 10^{-3}$	<i>ACTB, AZGP1, ALB, KRT1</i>

SRP-dependent cotranslational protein targeting to membrane	$1.91 \times 10^{-3}$	<i>RPL7, RPL15, FAU, RPS2, RPL29</i>
hemidesmosome assembly	$1.97 \times 10^{-3}$	<i>KRT5, KRT14, DST</i>
single organismal cell-cell adhesion	$2.48 \times 10^{-3}$	<i>JUP, DSG1, DSP, SHC1, CSTA</i>
anion transport	$2.70 \times 10^{-3}$	<i>VDAC2, VDAC3, VDAC1</i>
translation	$2.97 \times 10^{-3}$	<i>RPL7, SLC25A5, RPL15, SLC25A3, FAU, RPS2, RPL29</i>
viral transcription	$3.61 \times 10^{-3}$	<i>RPL7, RPL15, FAU, RPS2, RPL29</i>
regulation of anion transmembrane transport	$3.99 \times 10^{-3}$	<i>VDAC2, VDAC3, VDAC1</i>
cell-cell adhesion	$4.16 \times 10^{-3}$	<i>BSG, FSCN1, RPL15, RPS2, DBN1, ANXA2, RPL29</i>
nuclear-transcribed mRNA catabolic process, nonsense-mediated decay	$4.48 \times 10^{-3}$	<i>RPL7, RPL15, FAU, RPS2, RPL29</i>
translational initiation	$7.34 \times 10^{-3}$	<i>RPL7, RPL15, FAU, RPS2, RPL29</i>
cytoplasmic translation	$8.55 \times 10^{-3}$	<i>RPL7, RPL15, RPL29</i>
positive regulation of cell death	$1.14 \times 10^{-2}$	<i>PHB, HBA1, HBB</i>
ATP biosynthetic process	$1.14 \times 10^{-2}$	<i>LDHC, ATP5B, ATP5A1</i>
positive regulation of gene expression	$1.59 \times 10^{-2}$	<i>APOB, ACTA1, PHB, VIM, ZPR1, MSN</i>
regulation of heart rate by cardiac conduction	$1.64 \times 10^{-2}$	<i>JUP, DSP, AKAP9</i>
cell envelope organization	$1.67 \times 10^{-2}$	<i>HRNR, TGM3</i>
muscle filament sliding	$1.91 \times 10^{-2}$	<i>MYL6, ACTA1, VIM</i>
lipoprotein metabolic process	$1.91 \times 10^{-2}$	<i>APOB, APOE, ALB</i>

receptor-mediated endocytosis	$2.05 \times 10^{-2}$	<i>APOB, APOE, ALB, HBA1, HBB</i>
lipoprotein catabolic process	$2.22 \times 10^{-2}$	<i>APOB, APOE</i>
adenine transport	$2.22 \times 10^{-2}$	<i>SLC25A5, VDAC3</i>
keratinocyte migration	$2.77 \times 10^{-2}$	<i>KRT16, KRT2</i>
leukocyte migration	$3.11 \times 10^{-2}$	<i>APOB, BSG, SHCI, MSN</i>
peptide cross-linking	$3.19 \times 10^{-2}$	<i>DSP, TGM3, CSTA</i>
rRNA processing	$3.22 \times 10^{-2}$	<i>RPL7, RPL15, FAU, RPS2, RPL29</i>
response to hydrogen peroxide	$3.31 \times 10^{-2}$	<i>HSPD1, HBA1, HBB</i>
bundle of His cell-Purkinje myocyte		
adhesion involved in cell communication	$3.31 \times 10^{-2}$	<i>JUP, DSP</i>
lipoprotein biosynthetic process	$4.93 \times 10^{-2}$	<i>APOB, APOE</i>

**Table S4. The top 40 most-enriched functions of the genes that have a *P*-value less than 0.05 in the predicted signaling network regulated by DCF1 in HEK293T-TAT-DCF1, where the biological process from Gene Ontology was considered.**

**Table S5**

Function	<i>P</i> -value	Genes in the predicted signaling network
intermediate filament organization	$1.02 \times 10^{-3}$	<i>KRT9, VIM, KRT2</i>
viral process	$1.90 \times 10^{-3}$	<i>SLC25A5, KRT8, VIM, SHCI, HSPD1, VDAC1</i>

epidermis development	$2.07 \times 10^{-3}$	<i>KRT9, KRT5, KRT16, KRT2</i>
SRP-dependent cotranslational protein targeting to membrane	$2.75 \times 10^{-3}$	<i>RPL18, RPL14, RPL15, RPL29</i>
viral transcription	$4.51 \times 10^{-3}$	<i>RPL18, RPL14, RPL15, RPL29</i>
nuclear-transcribed mRNA catabolic process, nonsense-mediated decay	$5.34 \times 10^{-3}$	<i>RPL18, RPL14, RPL15, RPL29</i>
retina homeostasis	$6.31 \times 10^{-3}$	<i>ACTG1, ALB, KRT1</i>
translation	$6.73 \times 10^{-3}$	<i>RPL18, RPL14, SLC25A5, RPL15, RPL29</i>
protein stabilization	$7.72 \times 10^{-3}$	<i>PPIB, NAA16, HSPD1, GAPDH</i>
translational initiation	$7.87 \times 10^{-3}$	<i>RPL18, RPL14, RPL15, RPL29</i>
keratinocyte migration	$1.48 \times 10^{-2}$	<i>KRT16, KRT2</i>
membrane raft assembly	$1.77 \times 10^{-2}$	<i>FLOT1, ANXA2</i>
rRNA processing	$2.58 \times 10^{-2}$	<i>RPL18, RPL14, RPL15, RPL29</i>
chaperone mediated protein folding requiring cofactor	$2.94 \times 10^{-2}$	<i>HSPE1, HSPD1</i>
hemidesmosome assembly	$3.52 \times 10^{-2}$	<i>KRT5, DST</i>
anion transport	$4.09 \times 10^{-2}$	<i>VDAC2, VDAC1</i>
intermediate filament cytoskeleton organization	$4.38 \times 10^{-2}$	<i>KRT16, DST</i>
cell-cell adhesion	$4.68 \times 10^{-2}$	<i>RPL14, RPL15, RPL29, ANXA2</i>
regulation of anion transmembrane transport	$4.95 \times 10^{-2}$	<i>VDAC2, VDAC1</i>

**Table S5. The top 19 most-enriched functions of the genes that have a *P*-value less than 0.05 in the predicted signaling network regulated by DCF1 in U251-blank, where the biological**

**process from Gene Ontology was considered.**

**Table S6**

Function	P-value	Genes in the predicted signaling network
SRP-dependent cotranslational protein targeting to membrane	$3.89 \times 10^{-5}$	<i>RPL23, RPL14, RPL4, RPL28, RPS27A, RPS8, RPL29</i>
viral transcription	$1.04 \times 10^{-4}$	<i>RPL23, RPL14, RPL4, RPL28, RPS27A, RPS8, RPL29</i>
nuclear-transcribed mRNA catabolic process, nonsense-mediated decay	$1.45 \times 10^{-4}$	<i>RPL23, RPL14, RPL4, RPL28, RPS27A, RPS8, RPL29</i>
translation	$2.93 \times 10^{-4}$	<i>SLC25A31, RPL23, RPL14, RRBPI, RPL4, RPL28, RPS27A, RPS8, RPL29</i>
translational initiation	$3.11 \times 10^{-4}$	<i>RPL23, RPL14, RPL4, RPL28, RPS27A, RPS8, RPL29</i>
rRNA processing	$5.79 \times 10^{-4}$	<i>RPL23, RPL14, RIOK3, RPL4, RPL28, RPS27A, RPS8, RPL29</i>
DNA topological change	$1.54 \times 10^{-3}$	<i>HMGB1, HMGB2, TOP2A</i>
V(D)J recombination	$1.92 \times 10^{-3}$	<i>HMGB1, HMGB2, LIG1</i>
DNA ligation involved in DNA repair	$1.92 \times 10^{-3}$	<i>HMGB1, HMGB2, LIG1</i>
establishment of protein localization to plasma membrane	$2.74 \times 10^{-3}$	<i>ROCK1, FLOT2, SPTBN4, FLOT1</i>

apoptotic DNA fragmentation	$4.37 \times 10^{-3}$	<i>HMGB1, HMGB2, KPNB1</i>
intermediate filament organization	$4.98 \times 10^{-3}$	<i>KRT9, VIM, KRT2</i>
microtubule cytoskeleton organization	$1.19 \times 10^{-2}$	<i>SON, MAPT, PAFAH1B1, GAPDH</i>
positive regulation of interferon-beta production	$1.39 \times 10^{-2}$	<i>HMGB1, HMGB2, FLOT1</i>
adult walking behavior	$1.81 \times 10^{-2}$	<i>EFNB3, MAPT, SPTBN4</i>
DNA geometric change	$2.64 \times 10^{-2}$	<i>HMGB1, HMGB2</i>
negative regulation of cholesterol biosynthetic process	$3.29 \times 10^{-2}$	<i>ERLIN1, SCAP</i>
neuron migration	$3.32 \times 10^{-2}$	<i>NDE1, MAPT, DNER, PAFAH1B1</i>
membrane raft assembly	$3.94 \times 10^{-2}$	<i>FLOT2, FLOT1</i>
regulation of circadian rhythm	$4.23 \times 10^{-2}$	<i>MAPK10, TOP2A, FBXL3</i>
SREBP signaling pathway	$4.58 \times 10^{-2}$	<i>ERLIN1, SCAP</i>
regulation of microtubule motor activity	$4.58 \times 10^{-2}$	<i>NDE1, PAFAH1B1</i>

**Table S6. The top 22 most-enriched functions of the genes that have a *P*-value less than 0.05 in the predicted signaling network regulated by DCF1 in U251-TAT-DCF1, where the biological process from Gene Ontology was considered.**

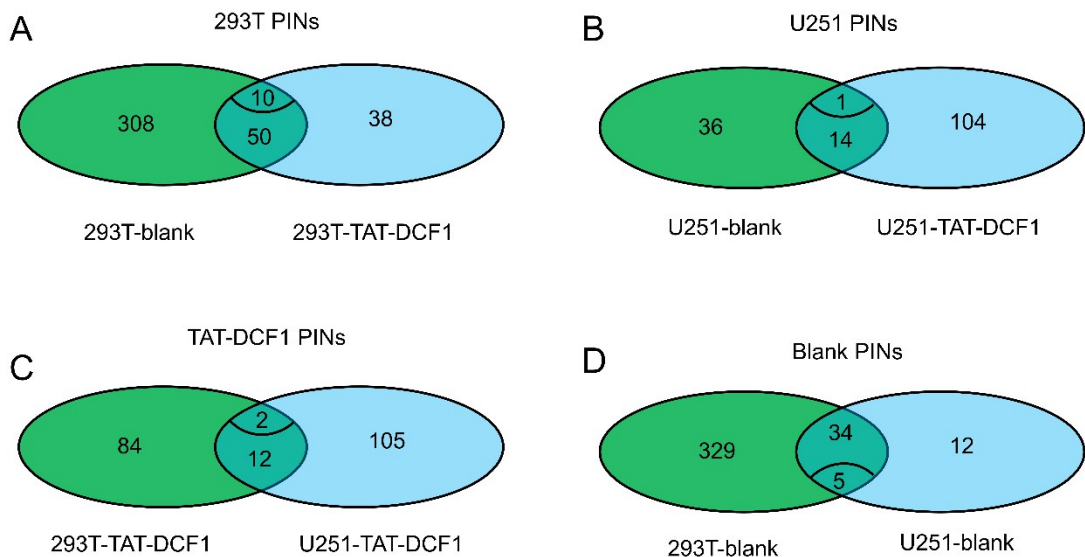


**Figure S1.** Protein numbers in PINs. The connected PINs were constructed based on the STRING database. HEK293T-blank, HEK293T-TAT-DCF1, U251-blank, and U251-TAT-DCF1 involved 368, 98, 51, and 119 proteins, respectively, among which the D values greater than 0.4 were selected and recognized as proteins with significant changes, which were 10, 1, 2, and 34, respectively.

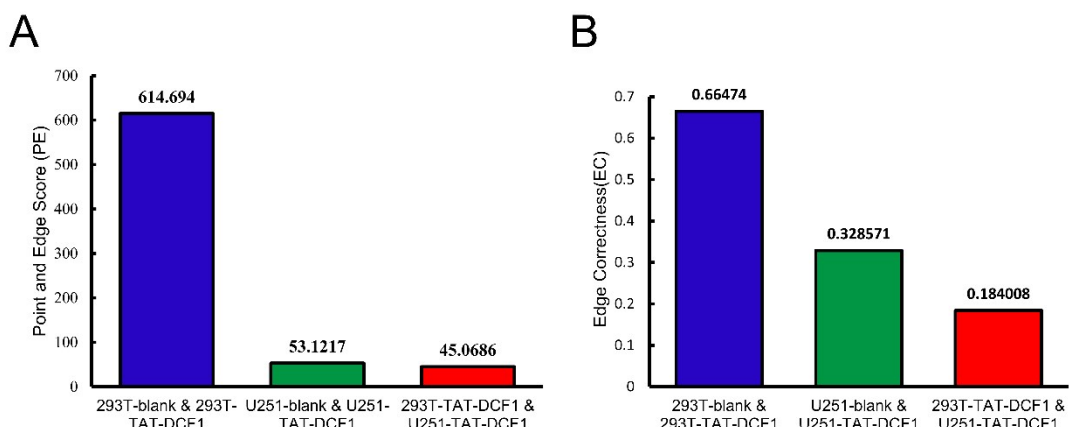
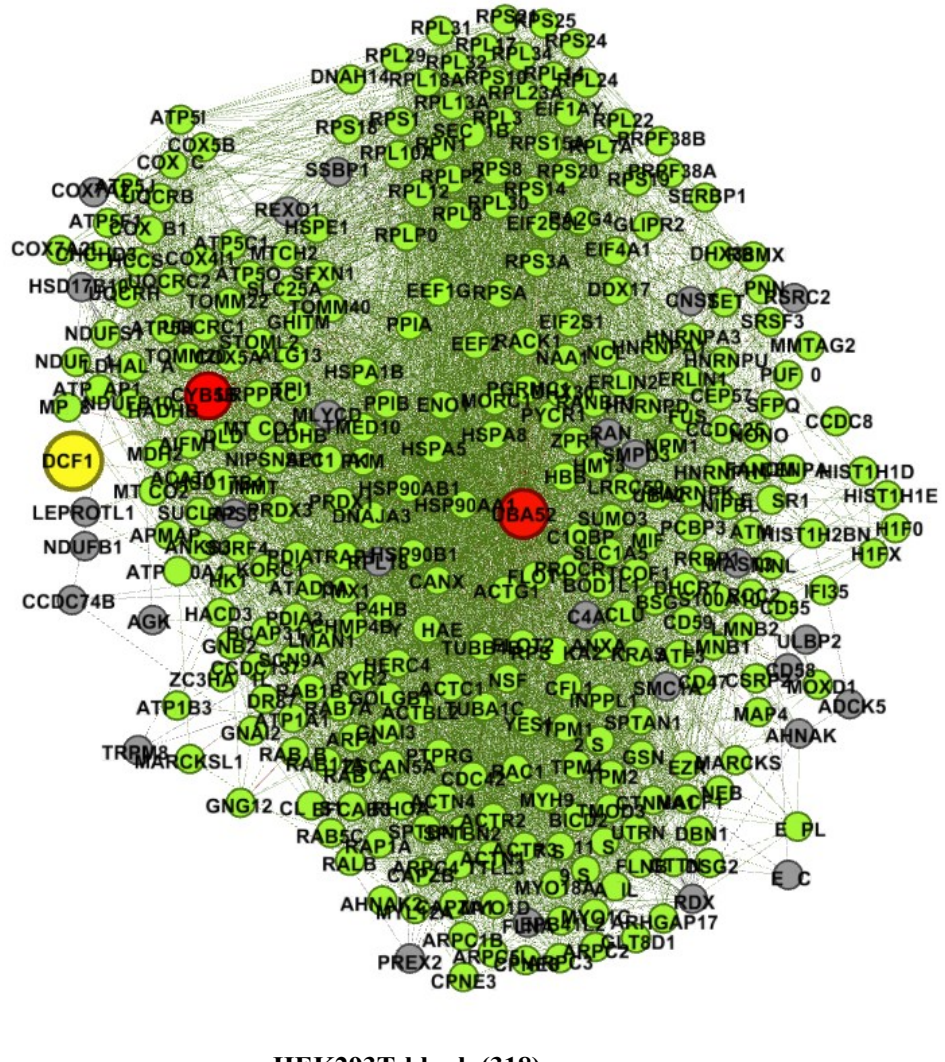


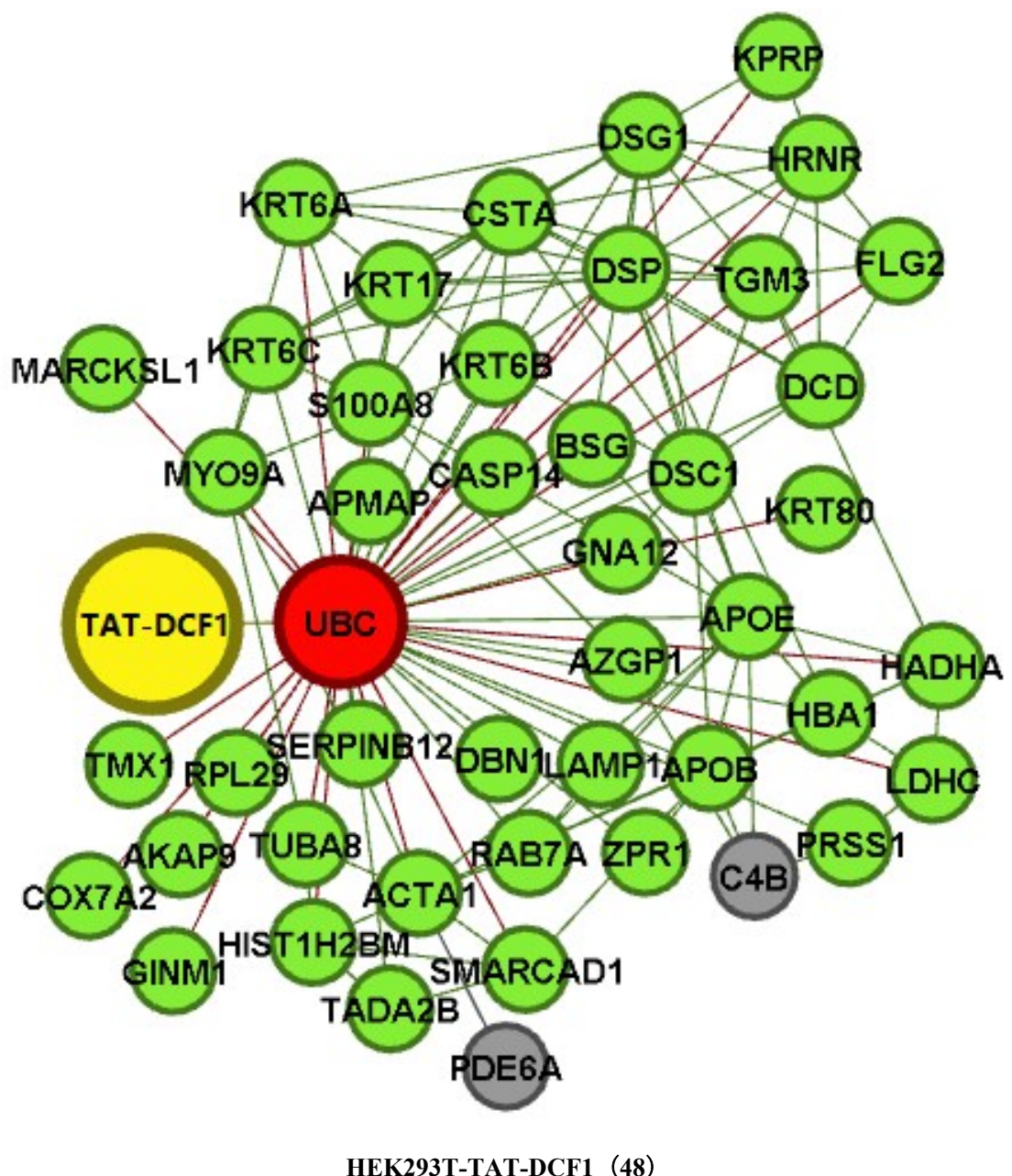
**Figure S2.** The PES and EC of the protein-protein interaction network.

**Figure S3**

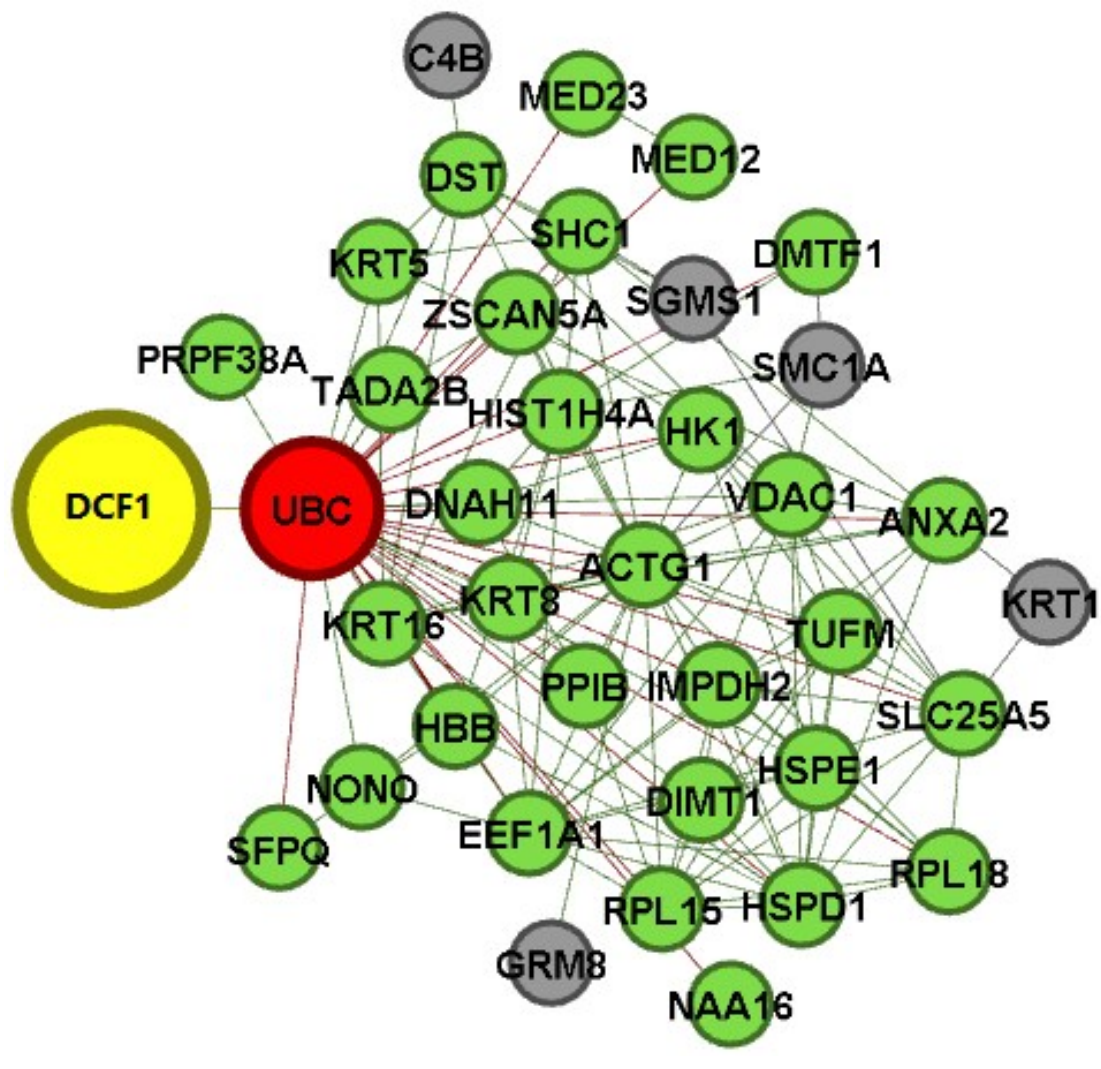
A



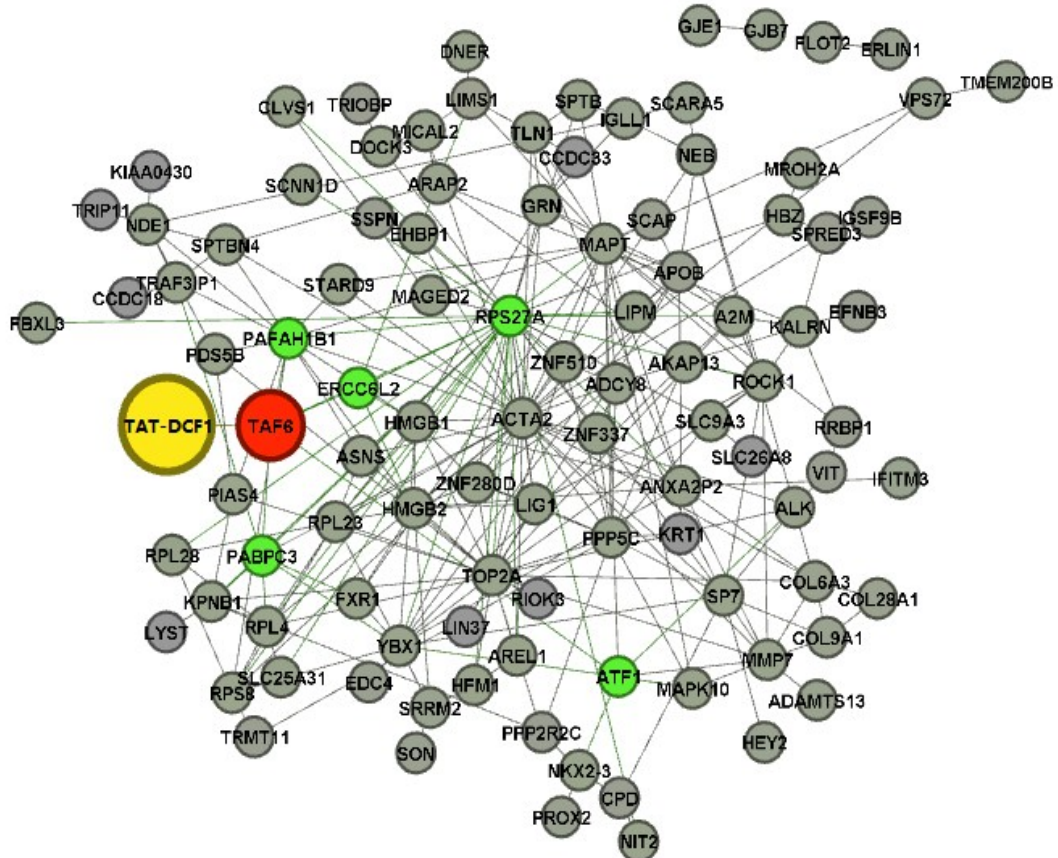
B



C

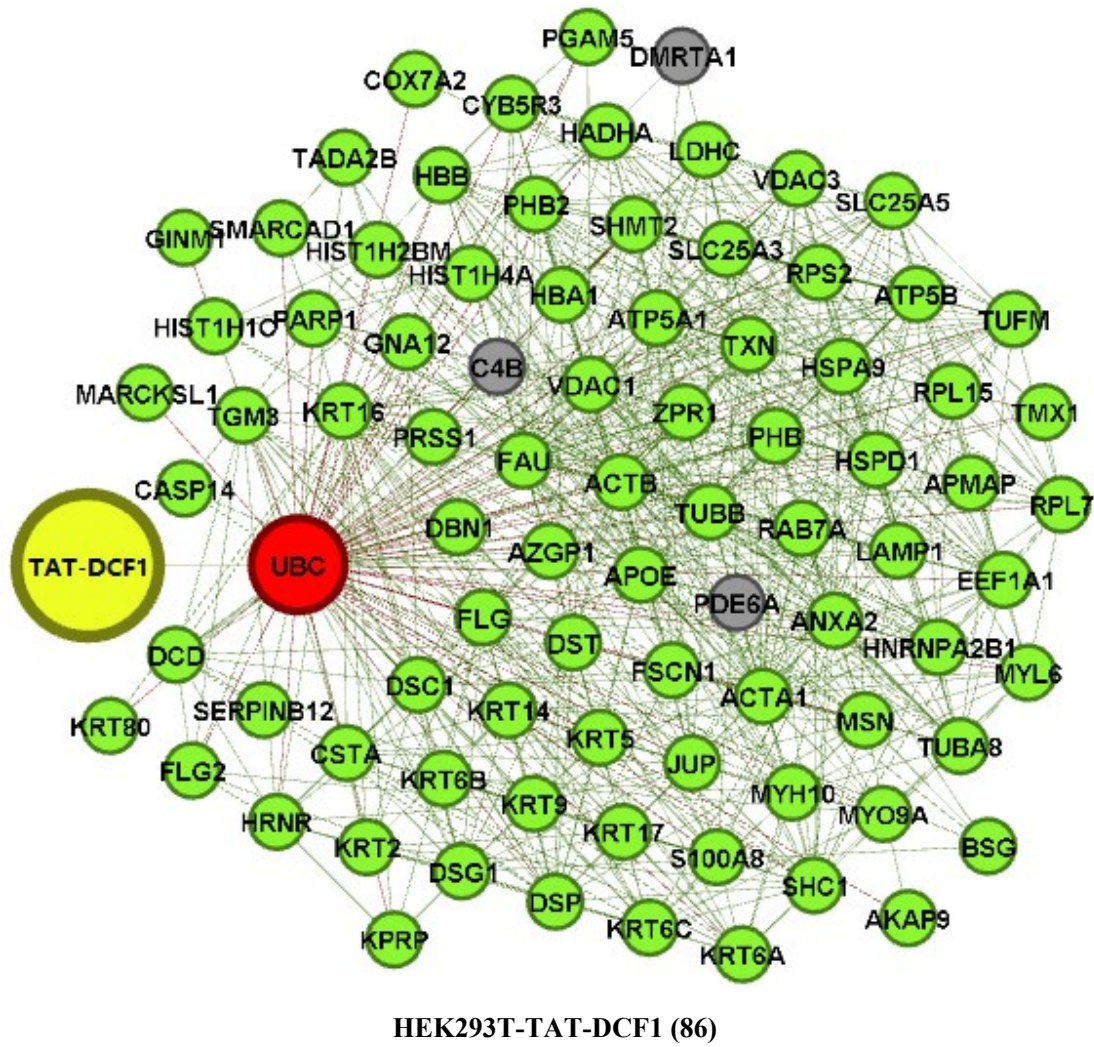


D

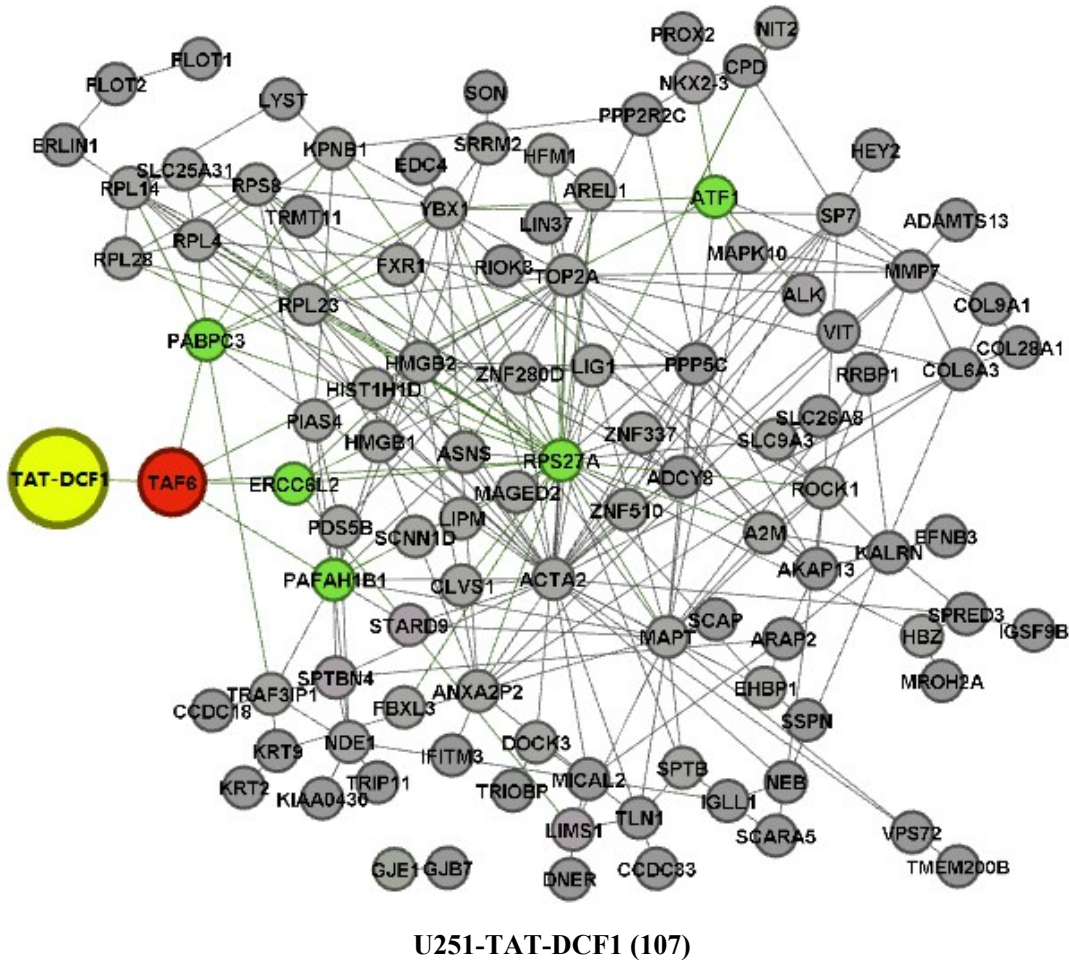


U251-TAT-DCF1 (105)

E



F



**U251-TAT-DCF1 (107)**

**Figure S3 Protein interaction networks induced by the TAT-DCF1 peptide in U251 and HEK293T cells. Networks were constructed through pairwise comparison between HEK293T-blank (318) (A) and HEK293T-TAT-DCF1 (48) (B) U251-blank (37) (C) and U251-TAT-DCF1 (105) (D), HEK293T-TAT-DCF1(86) (E) and U251-TAT-DCF1(107) (F).**

**The red nodes denote the genes that directly interact with the yellow nodes, and the green nodes denote the genes that directly interact with the red nodes.**